GEOFIZIKA VOL. 22 2005

Original scientific paper
UDC 551.578

Drop size distributions of tropical rain over south India

Soma Sen Roy, R. K. Datta, R. C. Bhatia and A. K. Sharma

India Meteorological Department, New Delhi, India

Received 6 December 2004, in final form 14 July 2005

Drop size distributions (DSD) associated with tropical rainfall at Cuddalore in the south-eastern part of India have been measured by a Joss-Waldvogel disdrometer (RD–80 model) during September to November 2002. The rainfall data corrected for instrumental error, matches very well with rainfall rates measured by a self recording raingauge, at the same site. For further analysis of the DSD, the rainfall events were separated into convective and stratiform rainfall by an algorithm based on variation of DSD parameters. One rain event in the form of a squall line of 15 September 2002, was analysed in greater detail to investigate the validity of the classification scheme as well as to study the variation of the DSD parameters during the course of a rain event. It was observed that, the algorithm was robust and had quite good correspondence with other independent rainfall separation algorithms. During the rain event, at low rainrates, the convective phase of the rainfall event was marked by DSD spectra that have greater population of small droplets as compared to stratiform DSDs at the same rainrates. At higher rainrates, the convective regime is characterised by narrow spectra centred at higher diameters. At the transition region between convective and stratiform spectra, mixed large and small drop spectra are observed. Similar variation was also observed in the averaged drop spectra. In addition, the averaged spectra also reveal an equilibrium distribution of the drop population in DSDs at higher rainrates (>39 /hr) for diameter range (>1.91 mm) corresponding to nearly constant values of the slope of the distribution, the intercept and the mean mass diameter. The value of the shape parameter, which for small rainrates varies the same as the slope parameter, starts to increase with increasing rainrate as the other two parameters of the gamma distribution approach a constant value corresponding to equilibrium shape. The value of the intercept parameter is highest for low to moderate convective rainfall and decreases as the rainrate increases.

Keywords: Convective, stratiform rainfall, disdrometer, deadtime correction, squall line, gamma distribution, drop coalescence, aggregation, riming

1. Introduction

October to December is the major period of rainfall in south India, particularly the eastern half of the peninsula. By October, a low pressure estab-

lishes itself over the central and southeast Bay of Bengal, moving southward as the season progresses. Under the impact of this low-pressure area, weather systems originate in the Bay of Bengal between 8 °N – 14 °N and influence the southern peninsula of India. Rainfall systems during this season, often called the northeast or winter monsoon season, are mainly of convective origin. The rain events last for several hours at a stretch and consist of both heavy showers for short periods as well as light uniform rainfall for longer periods (Srinivasan and Ramamurthy, 1973).

The process of raindrop formation, growth, transformation and decay occur on a microphysical scale within a large cloud scale environment. Each process such as condensation growth/evaporation or collision/coalescence leaves a signature on the drop size distribution (hereafter DSD) of the rain event. Hence analysis of the form of the DSD, its temporal and rainrate dependent evolution at the surface and also aloft, is essential in understanding the process of rainfall formation. Recent DSD studies have focussed on the differences between convective and stratiform rain, their differing characteristics and the physics of their formation. Houghton (1968) pointed out that the primary precipitation growth process in convective precipitation is a collection of cloud water by precipitation particles in strong local updraft cores. As the parcels of air in the convective updrafts rise out of the boundary layer and reach the upper troposphere, they broaden and flatten as a result of decreasing vertical velocity of the parcel and on reaching their level of neutral buoyancy, spread out and amalgamate to form a large horizontal area, which we identify as a stratiform region on the radar (Yuter and Houze, 1995). Under these conditions, the primary precipitation growth process is vapour deposition on ice particles formed earlier in the convective updrafts, but left aloft as the convective drafts weaken. It is a slow process, with particles always settling downwards.

In this study, we seek to categorize the one minute resolution DSDs of rain events obtained from a disdrometer into stratiform and convective rainfall, examine the robustness of the classification scheme, as well as understand the physical reasons for the corresponding spectral shape through analysis of their rainrate dependent variation as well as temporal variation during a rain event.

2. Data and instrumental setup

The raindrop DSD was measured with a RD–80 model disdrometer, which is an advanced version of the RD–69 model developed by Joss and Waldvogel (1967). A disdrometer (RD-80 model by Distromet Ltd., Switzerland) was installed at Cuddalore (11.43 °N, 79.49 °E) under the Indo–US project in April 2002 to measure the rainrate along with the DSD of tropical continental rainfall. The rainfall datasets used in the present study were collected at Cuddalore during September – November, 2002 and consist of 4269 individual 1 minute resolution spectra spread over 16 rainfall events during the season.

The disdrometer measures the downward displacement of the sensor body when a raindrop impacts the sensor surface with a sampling cross-sectional area of 50 cm^2. Raindrop diameters are sorted into 20 size intervals ranging from 0.1 to 5.0 mm. The number of counts in each of the 20 channels is recorded for a one-minute averaging period. One of the main problems of the RD-80 disdrometer (hereafter JWD) as with the RD–69 disdrometer, is its insensitivity to small drop population with diameter less than 1.0 mm during heavy rainfall (>20 mm/h). This causes underestimation of the small drop population during heavy rainfall events. This is known as the disdrometer's deadtime. Comparisons of DSD from a JWD with the raindrop spectra obtained from non-JWD sources by Loffler-Mang and Joss (2000) and Tokay et al. (2001) also indicate underestimation of raindrops for diameter range bins <0.7 mm by a JWD. For this reason, an algorithm has been developed by Waldvogel (personal communication) to mathematically correct this instrumental error during heavy rain, which is as follows:

$$N(i)^* = N(i) \exp\left[\frac{0.035}{T} \sum_{D(k)=0.85D(i)}^{D(k)_{\max}} N(k) \log_e \frac{D(k)}{0.85(D(i)-0.25)}\right]$$

Wherein $N(i)$ = number of drops in channel i without correction with diameter $D(i)$

$N(i)^*$ = corrected number of drops in channel i, k denotes the parameter values for channel with diameter greater than i and T is the sampling time in seconds. However, it may be noted that the algorithm is multiplicative. Hence if there are no drops in a given channel, the correction matrix does not add any drops to the given channel and modifies the DSD, thereby affecting the moments of the distribution. However, in all the rain events under review in this study, it is observed that for rainrates up to 51 mm/hr, almost all the DSD had raindrops in all the channels >0.40 mm, whereas up to 60 mm/hr all the DSD had raindrops in all channels >0.5 mm. As will be shown subsequently, the error due to underestimation of the raindrops in the lowest channels had very little effect on the higher moments of the DSD used to compute the integral parameters of the DSD.

Inspite of the deadtime correction algorithm, it is observed that as the rainrate increases, the distribution becomes progressively more skewed, and the number of droplets in the lower diameter categories decreases. However, observations from other sites (Sauvageot and Lacaux, 1995 (hereafter SL)) and from non disdrometer sources e.g. Fujiwara (1965), Cataneo and Stout (1968) and more recently, Jones (1992) using raindrop cameras have confirmed a strong lack of small drops at higher rainfall rates. Theoretical models (List and Gillespie, 1976; Brazier-Smith et al., 1973) also support these observations suggesting that the depletion of the smallest drops result from their collection by larger ones. In view of all the above observations, we inferred that the decrease in drop population in the lower diameter categories

is real and after the deadtime correction has been applied, the DSD represents, more or less, the actual drop population in different diameter categories. The actual DSD form will be investigated in greater detail in the subsequent sections. Also, according to Sheppard (1990), another instrumental problem of the JWD is due to some irregularities in the transfer function of the electronics used for the diameter classification of the raindrops of the JWD, which causes misclassification of the raindrops and producing erroneous peaks in the DSD. Corrections have however been incorporated into the diameter classification scheme of the data processing software (DISDROSOFT V 1.3) of the present instrument by the manufacturer and no pseudo peaks appear anymore in the DSD.

Ours, being an initial study at this location with this particular instrument (RD-80), it is essential to determine the accuracy of the instrument in measuring the observed rainrate. The rainrates calculated from the DSD measured by the JWD were compared to the values measured by a self recording rain gauge (SRRG) at the same site. Figure 1 shows the relative positions of the JWD and the SRRG at Cuddalore. The JWD is actually about 25 m to the east of the SRRG. Both instruments are in an open area away from the observatory. They are sheltered from strong winds by tall trees in the periphery of the observation site. Acoustic noise that causes error in DSD measurement by the JWD has thus been minimised.

Figure 1. Picture of the disdrometer site, showing relative positions of the JWD and the raingauge. The JWD is installed in the foreground while the raingauge may be observed in the background in blue inside the fenced in observation area. The JWD is actually about 25 m to the east of the SRRG.

It was observed that in case of heavy, short rain spells, when the rainrate is very high, the correspondence between the rainrate measured by the JWD and the SRRG becomes poorer. It may be that, the inertia of the pen on the chart recorder in case of the SRRG, does not permit it to record accurately the start and end times of very sharp, short spells of rain. Hence these start and end points of the rainfall period, measured by the SRRG are eliminated. Another problem encountered, with respect to SRRG measurement of rainrate, is due to duration of the rainfall. In case of very short spells of rain, time measurement from chart involves error, as the smallest division from the chart represents 15 minutes. Hence, only such rain events, extending for periods longer than 15 minutes, wherein the rainrate does not rise or fall very abruptly were considered for comparative analysis. The JWD rainrates for the period were averaged for 15-minute intervals corresponding to the period of measurement of the SRRG and the two measures of rainrate compared. Figure 2 demonstrates the regression relation between the two sources of measurement. The least square fitting of the two measurements is very close:

$$R = 0.99\ R_{SRRG}$$

where R : the rainrate measured by the JWD (mm/hr)
R_{SRRG} : the rainrate measured by the self recording rain gauge (mm/hr)

The correlation between the two is also very high (0.99). It may be noted that without the deadtime correction, the rainrate measured by the JWD is considerably lower (about 11%).

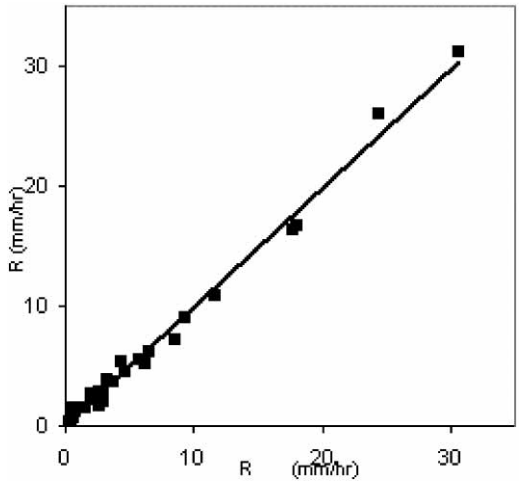

Figure 2. Comparison of rainrates R (mm/hr) measured with the JWD and R_{SRRG} (mm/hr) measured with a self recording raingauge. The bold straight line is the least square fitted curve to the data while the thin line signifies the 45° line for equal R and R_{SRRG} values.

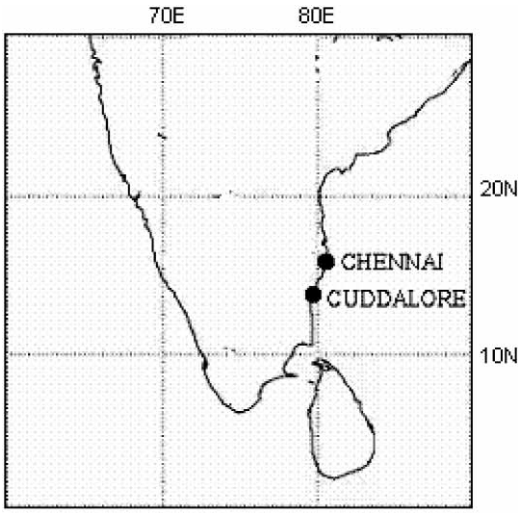

Figure 3. Location of the JWD site and the Radar site in India. The S-Band Doppler radar is about 160 Km. to the north of the JWD site.

Hence we conclude the deadtime correction algorithm is effective, and the corresponding corrected DSDs are further investigated. The structure of the rain events was also analysed using the reflectivity pictures of the S-Band Doppler Radar at Chennai (formerly Madras 13.04 °N, 80.17 °E) which is about 160 km. from the JWD site. Figure 3 displays the relative positions of the JWD site and the radar site.

3. Results and discussion

3.1. Classification of rainfall type

One of the major objectives of the study of the tropical precipitation is the determination of its relationship to the heating and large scale mass field and the resulting influence on the general circulation. As the mass field responds differently to the latent heating profiles in convective and stratiform precipitation, the two rainfall types should be separately analysed (Houze, 1993). However, it is difficult to establish an objective rainfall classification methodology.

According to the physical characteristics of the convective – stratiform clouds, precipitation type can be identified with the help of simultaneous observations of vertical air velocities and terminal fall speeds of hydrometeors (Houze, 1993). Since, until recently, these observations have been rare (Atlas et al., 2000; Yuter and Houze, 1995c; Tokay et al., 1999; being some examples), indirect methods have been developed based on various observed prop-

erties of convective and stratiform clouds, mostly based on the reflectivity echo pattern as measured by surface weather radars (Churchill and Houze, 1984; Steiner et al., 1995). However, due to interregional and interevent variation of the structure of rainfall giving clouds, no general model for separation of type of rainfall has been found to be acceptable to all. With the availability of reliable JWD observations of rainfall DSD, this became a major tool for identifying cloud types from rainfall received on the ground. Most studies of rainfall DSDs have observed a sudden decrease in the value of the intercept parameter N_0, for exponential and gamma DSD in association with transition of rainfall type from convective to stratiform. This result was first reported by Waldvogel (1974) and has since been consistently observed for tropical rainfall by various authors (Maki et al., 2000, (hereafter MKSN); Donnadieu, 1982). Recent studies by Heinrich et al. (1996) also demonstrate a clear relationship between the riming process in clouds and N_0 of the raindrop spectra, all of which change dramatically as riming increases, at times without a corresponding change in the rainrate. On the other hand, Stewart et al. (1984) have demonstrated the presence of large raindrops associated with the aggregation mechanism above the bright band in stratiform rainfall regions. Since riming (an indication of updrafts and convection) is the main process determining the form of the DSD in convective clouds, and aggregation is the most important process in stratiform DSD formation (Atlas and Ulbrich, 2000 (hereafter AU2000)), one may logically associate small drop DSD spectra (large N_0 values) with convective clouds and large drop spectra (small N_0) with stratiform mode of DSD formation, at the same rainrate. Following the physical arguments of Waldvogel (1974), Tokay and Short (1996, (hereafter TS)) found that the relation $N_0 = 4 \times 10^9\ \mathrm{R}^{-4.3}$ was a good threshold to distinguish between convective and stratiform precipitation in tropical oceanic rainfall. Tokay et al. (1999) compared this JWD based algorithm with the 915 Mhz wind profiler based rainfall separation method developed by Williams et al. (1995) and found reasonable agreement between the two methods for tropical oceanic rainfall.

The suitability of the application of the TS algorithm to the present study for the separation of the rain events into convective and stratiform rainfall episodes on the basis of DSD parameters has been investigated in this section through a few examples. The one-minute resolution DSDs were modelled using the modified gamma distribution analytical function. The modified gamma DSD (or three parameter DSD) proposed by Ulbrich (1983), used to model the distribution is of the form given below:

$$N(D) = N_0 D^{\mu} e^{-\lambda D}$$

The parameters of the distribution N_0, μ and λ are the intercept parameter, shape parameter and slope parameter of the fitted DSD respectively and have been computed by a method of moments (Ulbrich and Atlas, 1998 (here-

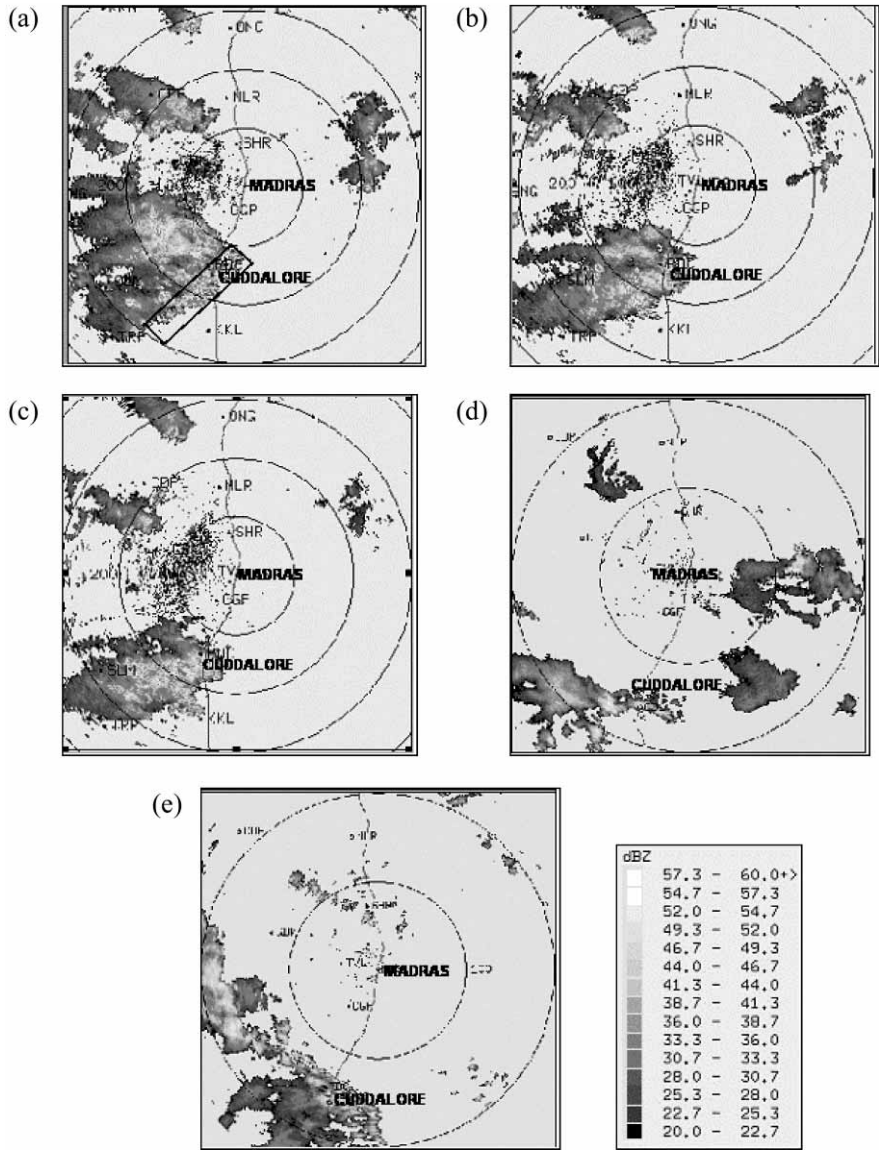

Figure 4. S-Band Doppler Radar PPI (Z) images at 0.2 degree elevation over Cuddalore during various rain events. Madras(Chennai) is the location of the radar which is 160 Km north of Cuddalore. Each circle denotes 100 km. range about Chennai. (a) 19:00 IST on 15 September 2002, when the leading convective edge of the squall line as enclosed by the rectangular box was over the station. (b) 20:00 IST on 15 September 2002 when the squall line is recurving and the reflective trough is over the station. (c) 20:30 IST on 15 September 2002 secondary high in the reflectivity, corresponding to the main stratiform region is over the station. (d) 03:30 IST on 18 September 2002, when a convective cell was over the station. (e) 23:43 IST on 10 October 2002, when the leading convective edge of the squall line was over the station.

after UA1998)), without truncation at the maximum drop diameter. Gamma distribution fitting has been done only for DSDs for rainrates more than 0.5 mm/hr, as below this rainrate, erratic results are obtained.

Case 1: A squall line rain event of 15 September, 2002 comprising both heavy and light showers over the station 18:31 IST to 21:14 IST is analysed. IST signifies the Indian Standard Time, which is five and a half hours ahead of UTC. The accumulation during the event was 43.6 mm and the peak rainrate associated with the heavy rainfall regime, measured by the JWD is 101.8 mm/hr. The squall line was observed in the radar pictures (figure 4(a), (b) and (c)) as a northeast –southwest oriented band of high reflectivity, that moved in a south easterly direction to over the observation site, before recurving and moving south-westwards and then finally losing its distinctive form and ending its life as a cloud cluster south of the station.

Figure 5 displays a line diagram of R vs. N_0. It may be observed from figure 5, that there is a clear separation of the N_0 value into two groups, one corresponding to continuous, low intensity long period rainfall and the other, the high intensity, short period rainfall. Hence the TS classification may be considered applicable to this particular rain event. However it may be noted, that the value of N_0 – R relationship (as indicated in figure 5 by the heavy grey line), that separates the entire event into two rainfall types is given by $N_0 = 5.8 \times 10^7\ R^{-4.45}$, which is about hundred times lower than the value obtained by TS. This may be because, TS employed the third, fourth and sixth moments of the DSD in determining the parameters of the gamma distribu-

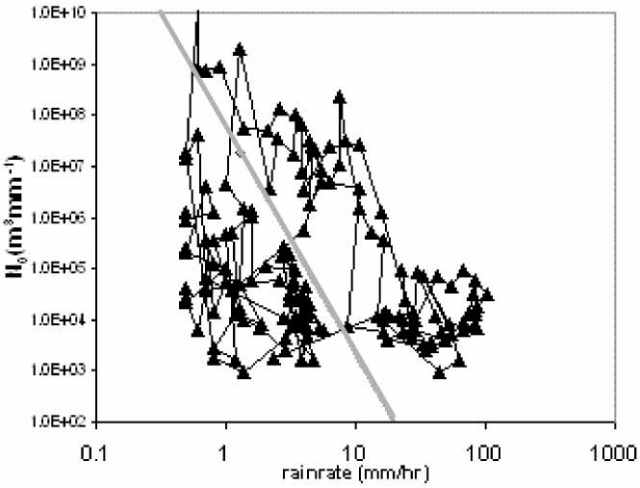

Figure 5. A case study of the squall line of 15 September 2002. Intercept parameter N_0 (m^{-3} mm^{-1}) of the gamma drop size distribution as a function of the rainfall rate. The solid line indicates the value of $N_0 = 5.8 \times 10^7\ R^{-4.45}$ that separates the event into two contiguous groups of data points.

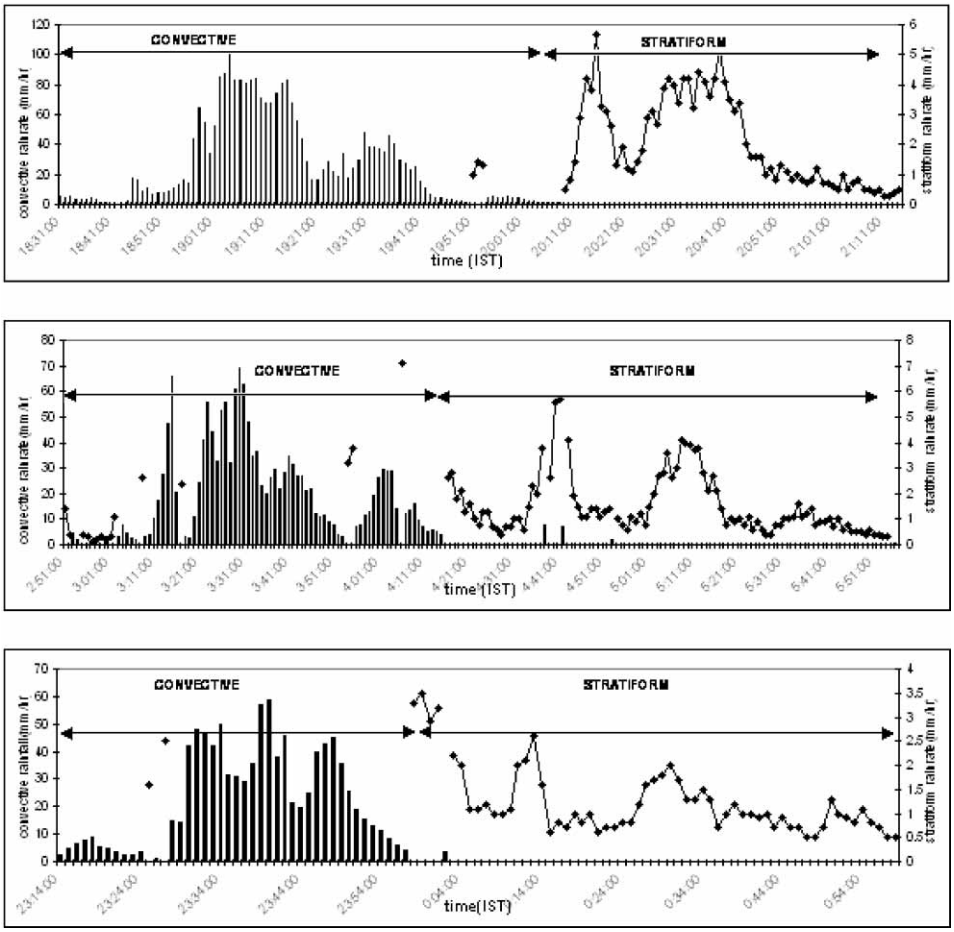

Figure 6. Time series of the rainrates for three rain events: (a) A squall line event on 15 September 2002 (b) A convective system on 18 September 2002 (c) A squall line event on 10 October 2002

tion; whereas in the present study, the second, fourth and sixth moments of the DSD have been employed following the UA1998 study. All the three parameters of the gamma distribution are very sensitive to the moments of the raindrop spectra. The relation between the intercept parameter and rainrate is therefore expected to be different than the TS study.

The corresponding temporal variation of the classification scheme may be observed in figure 6(a). The columns indicate convective rainfall. Since stratiform rainrates are very low compared to convective rainrates, a scale change has been effected for the stratiform rainrates as indicated by the line with solid circles. The convective classification was predominant in the ini-

tial light rain, as well as the heavier showers that followed until 20:09 IST, when the leading convective line and then the transition region was directly over the station. The rainfall became predominantly stratiform thereafter, up to 21:14 IST at the end of the rainfall event corresponding to the presence of the secondary maximum in reflectivity over the station.

The columns indicate convective rainfall. A scale change has been affected for the stratiform rainrates as indicates by the line with solid circles.

Case 2: A widespread cloud patch was observed in the neighbourhood of the station, on 18 September 2002. The entire low reflectivity cloud mass was moving in a south eastward direction, while short lived very intense convective cells formed and decayed in this cloud cluster. The actual rainfall extended intermittently from 20:30 IST of 17 September to 05:37 IST of 18 September. However, in figure 6(b) we have displayed a part of the total time series starting when a convective cell was directly over the station (figure 4(d)) at 03:30 IST. There was very little rainfall (<0.5 mm/hr) in the preceding two hours and this rainfall spell started at 02:51 IST with predominantly convective rain on the ground corresponding to the high reflectivity convective cell overhead. At 04:15 IST the rainfall changed to stratiform and continued to be so till the end of the rainfall period.

Case 3: A north-west south-east oriented squall line on the night of 10 October 2002 was observed in the neighbourhood of the station moving in a north-easterly direction. The figure 4(e) displays the PPI reflectivity picture of the position of the squall line at 23:43 IST, when the leading convective edge was just over the station. Rainfall occurred for a total of one hour 44 minutes from 23:14 IST of 10 October to 00:58 IST of 11 October. Peak rainfall was 62.5 mm/hr while the total accumulated rainfall was 18.23 mm. As displayed in figure 6(c), the convective classification was predominant in the initial light rain until 23:27 IST followed by heavier showers until 23:57 IST, when the leading convective line was directly over the station. Following the convective line, the separation of the transition and stratiform regions are not evident unlike the first case, and the trailing low reflectivity region was observed to give predominantly stratiform rainfall on the ground upto the end of the rainfall period.

The above classification scheme has been applied to all kinds of rainfall events during this season, both from single cumulus cells as well as multicellular complex cloud structures. Although, the jump in the value of N_0 is not so unambiguous in all rainfall events of this study, it is observed that this $N_0 - R$ relation best separates the rainfall DSD of most rainfall events into temporally contiguous groups, identified here as convective (above) and stratiform (below the bold line in figure 5). Minute to minute variations in classification can be seen occasionally in the time series revealing the empirical nature of the method. However the classification is quite stable. A 10 % change in the slope or intercept of the $N_0 - R$ relation brings about only a 2–3% change in the classification scheme.

3.2. Temporal variation of DSD parameters during a rainfall event

While the different phases of the rainfall in the above events, have been broadly categorized as convective and stratiform type using the modified TS algorithm in the previous section, given the complexity of structures observed in tropical precipitation substantial systematic temporal variation of the DSD parameters is often observed within a rainfall event, even for the same rain type and rainrate, depending upon the location of the DSD in the overall rain event.

The rain event discussed above in case 1, was analysed in greater detail in order to study the robustness of the above classification scheme and also investigate the structure of a squall line as it moved over the station. Radar images at 15 minute intervals from the Doppler radar at Chennai (radar

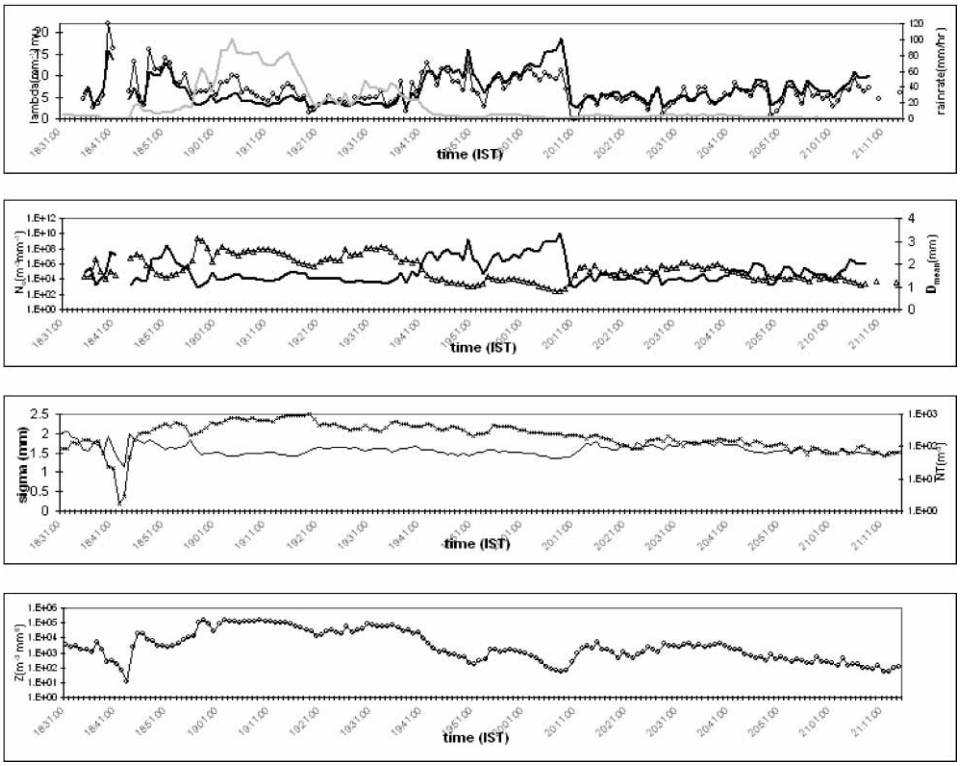

Figure 7. Same case study of 15 September 2002, indicating variation of the different DSD parameters with rainrate (a) μ (hollow dotted curve) and λ (mm^{-1})(bold curve) (b) N_0 (m^{-3} mm^{-1}) (bold curve) and D_{mean} (mm) (hollow triangles curve) (c) N_T (m^{-3}) (cross hatched curve) and σ (mm) (bold curve) (d) Z ($m^{-3}mm^6$) (hollow dotted curve)
For comparison purposes the corresponding temporal variation of rainfall (mm/hr) is also displayed in light curve in figure 7(a).

beamwidth 1°) were analysed to understand the structure of the squall line as it moved over the station and to corroborate the rainrate variation on the ground with the reflectivity variation aloft. Three such radar reflectivity pictures, corresponding to the different phases of the squall line over the station, have been displayed in figure 4(a), (b) and (c) respectively.

In addition to the three parameters of the fitted gamma distribution *i.e.* N_0, μ and λ, the temporal variation of two more parameters of the DSD, namely N_T and σ were also analysed. N_T signifies the total number of raindrops in the DSD while σ is the standard deviation of the DSD about the geometric mean diameter (Feingold and Levin,1986). These parameters do not require the assumption of a specific form of the DSD (gamma distribution as in the method of moments) (UA 1998, Atlas et al., 2000) and hence give actual estimates of the DSD characteristics. In fact, studies have shown that the standard deviation of the spectrum may be considered a better estimate of the spectrum width as compared to the gamma distribution shape factor, whose value may be erroneously large when the method of moments is applied (UA 1998). Besides the above parameters, a sixth parameter, *i.e.* mean mass diameter$_{mean}$ (mm) is also computed for the DSD. It is the ratio of the fourth and third moments of the DSD. The value of this parameter, in combination with , provides information of the asymmetry (skewness) of N(D). The seventh parameter, whose temporal variation with the rainrate is also simultaneously studied, is the JWD-measured reflectivity. The temporal evolution of all the above parameters is displayed in figure 7 (a), (b), (c) and (d).

The initial rain rate over the station is very low. A few minutes before the leading edge of the main heavy spell arrived over the JWD site, the value of most DSD parameters namely N_0, μ, λ, N_T and σ change without a corresponding variation in the rainrate. The increase in the value of N_T and σ without a corresponding rise in the value of D_{mean} (which in fact decreases) or the rainrate indicates that the spectrum broadening is mostly due to increase in the drop population in the smaller diameter categories which do not substantially affect the rainrate (Uijlenhoet, 2003).

Within this convective region, the rainrate then rises very steeply and there is a very heavy shower over the observation site from 18:45 IST to 19:48 IST. Radar reflectivity pictures (figure 4(a)) reveal that during this period, an extended line of deep convection with corresponding high reflectivity values was over the station. This region is marked by organised multicellular structure, (enclosed in the bold rectangular box), and is often called the leading convective line of a squall line event (Smull and Houze, 1987). Corresponding to the leading edge of this convective line, from 18:56 IST to 18:58 IST the rainrate increases sharply, and there is a corresponding sharp increase in the value of D_{mean} (3.0 mm) without a corresponding increase in the number concentration N_T, over the previous high value. It is observed that, steeper the leading edge of the convective spell, larger is the increase in the value of D_{mean}, a magnitude not generally observed for the corresponding

rainrate in any other part of the spectrum. The variation of the above parameters, seen together, indicates a narrow peaked DSD (decreases with increasing rainrate), skewed towards higher drop diameters during this phase of the event. Beyond the leading edge is the convective centre region which MKSN defined as the region immediately following the leading edge, wherein the rainrate >20 mm/hr, which in this case extends from 18:58 IST to 19:40 IST. The value of D_{mean} decreases slightly from the value at the leading edge (between 2.2 mm and 2.7 mm), and its rainrate dependent change becomes less obvious, especially for rainrates (>40 mm/hr). The reflectivity values for the DSD are also observed to become almost constant, independent of the rainrate, especially above 40 mm/hr rainrates. As the rainrate increases, N_0 as well as λ appear to be inversely related to the rainrate, but the rate of change decreases at higher rainrates, especially beyond 40 mm/hr. On the other hand, with increase in the rainrate, the value of the shape parameter, which for small rainrates varies the same as the slope parameter, starts to increase with increasing rainrate.

At the trailing edge of the convective spell, from 19:41 IST to 19:48 IST, the rainrate decreases more slowly, and there is a corresponding drop in the value of D_{mean}. The total number concentration of the particles, N_T, also decreases, but the decrease does not correspond very well to the rainrate decrease and is relatively high, even when D_{mean} as well as the rainrate has decreased to a minimum value. When seen in conjunction with increasing values of σ, it indicates a broadening of the DSD spectrum and a gradual increase in the low drop diameter population at the expense of the large drop population.

The transition of the DSD within the convective spell, from the broad spectrum small drop intensive regime at small rainrates, at the edges of the convective spell (mainly the trailing edge), to a narrow, skewed, large drop regime during the main convective spell, appears to validate the models for convective storms proposed by various authors. Investigation of the structure of tropical squall lines over Florida from NCAR Electra aircraft flights show that, the centre of the convective cloud core is a region of high reflectivity and is characterized by strong local updrafts, which occur intermittently and sporadically (Yuter and Houze, 1997). The sharp increase in the value of D_{mean} with increase in the rainrate indicates strong low-level growth, evaporation or both in the convective region in this updraft region (Atlas et al., 1999 (hereafter AUMAW)). A model for convective storms in the TOGA-COARE experiment, proposed by AU 2000, suggests that the updraft regions produce small drops through collision break-up, which are removed by updraft winds from the final DSD before they reach the ground. Hence large droplets produced by coalescence are predominant in the ground spectra of the convective centre region of the storm. The detrained smaller droplets (or more generally hydrometeors) travel upward and outward and fall out in the outer edges of the cloud, forming broad, small drop spectra where the vertical updrafts are

weaker. These updrafts are stronger at the leading edge (Yuter and Houze, 1995). Hence there is greater sorting, resulting in a sharp peak in the mean mass diameter. The small drop population at the trailing edge of the convective event increases with time, as the updrafts gradually decrease in strength, away from the convective centre. As the storm begins to fade, the reflectivity as well as the rainfall decreases in the wake of the storm. According to Yuter and Houze (1995), the storm is decaying at this stage, wherein, however the vertical velocities associated with the decaying convection are still strong enough. The detrained particles of the convective storm at different layers now gradually fall out as the vertical velocity decreases. Those particles detrained in the warm regions are liquid droplets. As they fall, they are subject to general drop size decrease due to evaporation in the dry upper atmosphere and also loss due to subsidence. The above process least affects the particles detrained in the lower levels; while the drops detrained in the upper atmosphere suffer the most. This may explain the gradual shift of the entire DSD to smaller raindrops with time at the trailing edge of the main convective line; accompanied by broadening of the DSD spectrum due to large concentration of droplets, not commensurate with the rainrate.

Following the trailing edge of the convective spell, the rainrate as well as the reflectivity is observed to decrease to very low values from 19:49 IST to 20:09 IST. Mean mass diameter D_{mean} is quite low at the end of the heavy shower and is nearly constant at about 1.0 mm. Radar pictures (figure 4(b)) show the leading edge of the squall line breaking up as it recurves and moves southwards from over the station. Over the station, a region of decreased echo intensity is observed, separating the leading convective line from the trailing stratiform region. This may be defined as the transition region on the basis of reflectivity pictures according to the definition by Smull and Houze (1987) and as the reflectivity trough by MKSN; though some authors have categorized such a region as initial stratiform region on the basis of variation of D_{mean}(AUMAW). This zone is characterized by deep subsidence at mid and upper levels. The corresponding DSD spectra are dominated by fallout of smaller particles (larger lower level detrained liquid droplets having already fallen out at the trailing edge, wherein the updrafts are less strong) (Uijlenhoet et al., 2003). The gamma DSD parameters in the present study, show a rainrate dependent behaviour, increasing as the rainrate decreases. Different authors have observed big or small drop spectra in this region. While AUMAW as well as MKSN observed this region to be composed mainly of large drop spectra, Uijlenhoet et al. (2003) observed the N_0 jump at the end of this period, indicating the small drop dominant character of the DSD in this phase of the event. In our study too, this region is characterized as convective, indicating the small drop character of this region. Yuter and Houze (1997) observed from NCAR Electra aircraft flights into convective storms, that in this fallout zone of a rain event, ice particles above the freezing level aggregate discontinuously and form much larger particles in the

DSD on the ground without necessarily increasing the rainrate. Whether or not aggregation takes place during this phase depends on a mixture of conditions, namely the size, shape and concentration of the ice particles, as well as vertical velocities in the air column over the station (Braun and Houze, 1994). In the absence of aggregation, riming is the only active process, which produces the characteristic small drop spectra (Heinrich et al., 1995). Hence this region is associated with small drop spectra. The rainrate being almost constant, when the DSD spectrum change from one type to another, a corresponding sharp change is observed in figure 7, in the value of the parameters N_0 (the N_0 jump) and to a lesser extent, the slope parameter λ. In the present study, one such »jump« is observed in the value of the DSD parameters at 19:50 IST and another at 20:09 IST, at the end of the transition period, as the rainfall changes from small drop convective to large drop stratiform type.

The rainfall region that follows this transition phase from 20:10 IST to 21:14 IST is generally characterised by exceptionally large and uniform values of reflectivity as well as D_{mean} (~1.9 mm), not commensurate with the rainrate for this phase of the rain event. Most studies, including the modified TS algorithm adopted in this study, characterize this region as the main stratiform region. The radar reflectivity PPI scan (figure 4(c)) too indicates a secondary maximum of radar reflectivity following the convective line during this period over the observation station. This region is characterized by mesoscale updrafts in the upper troposphere above the bright band and mesoscale downdrafts in the lower atmosphere (Yuter and Houze, 1997). In our study the values of the gamma DSD parameters *i.e.* N_0, μ and λ, are less than those for convective rainfall at the same rainrate. The predominance of the large drop spectra in the stratiform region indicates the relative importance of the aggregation mechanism of drop formation in this part of the rain event as proposed by Biggerstaff and Houze (1991). The behaviour at the large-drop end of the spectrum can be microphysically explained by the aggregation of ice particles above the freezing layer, in the presence of mesoscale low updrafts, which promote this process by increasing the residence time of the hydrometeors. These drops, upon melting, produce larger raindrops at the expense of intermediate ones. The sharp increase and thereafter uniform value of D_{mean}, σ and the reflectivity (JWD measured) without a corresponding rise in the rainrate also indicates significant evaporation in this region (Atlas and Chmela, 1957). The droplet size decrease due to evaporation and subsidence mainly affect the smaller drop end of the spectrum, thereby broadening the spectrum further by increasing the population of the small drops (AUMAW).

3.3. Variation of DSD parameters with rainrate

It may be inferred from the previous sections, that the modified TS algorithm adopted in the present study is quite robust and hence may be used to

further analyse the general nature of convective and stratiform spectra. In order to obtain significant estimates of the parameters describing the DSDs that can be compared with theoretical results, it is necessary to average the instantaneous DSDs in order to eliminate the randomly varying components and to obtain stable values of the DSD parameters differentiating convective and stratiform DSDs.

However, the previous sections also suggest that while convective rainfall dominates at higher rainrates, lower rainrates are mostly stratiform. In fact, when the convective–stratiform classification presented above was examined for 4269 DSDs spread over 16 events in figure 8, it was found that stratiform type of rainfall dominated the total number of rainfall DSD below 1 mm/hr (79%) while convective rainfall dominated beyond 10 mm/hr (99%). The two types of rainfall are more equally divided between 1–10 mm/hr. When all the DSDs corresponding to a single type of rainfall are grouped together irrespective of the rainrate and attempt is made to establish a single averaged or modal value of the rainfall parameters, we may unintentionally ascribe qualities to the rainfall type, which may actually be due to variation in the rainrate. This may hamper our understanding of the physics of occurrence of such rainfall. Hence the instantaneous DSDs of each rainfall sample during the period of observation were grouped into small classes of 3 mm/hr width from 1 mm/hr to 60 mm/hr for both types of rainfall. The number of samples in each class is indicated in figure 8. The average DSDs were calcu-

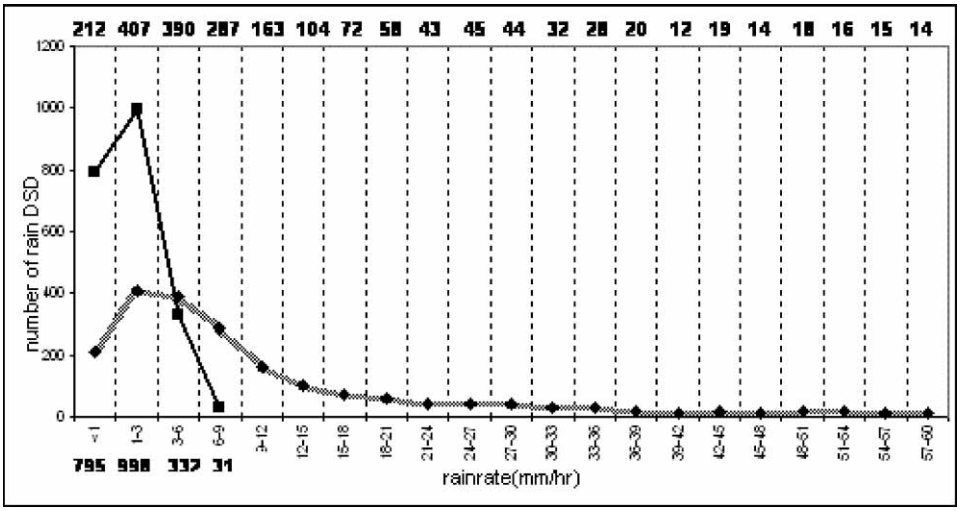

Figure 8. Number of DSD samples for each type of rainfall and as a function of the rainrate. The light curve indicates the number of convective rain samples while bold curve displays the same for stratiform rain events. The number of stratiform (convective) rainfall samples per 3 mm/hr of rainrate are indicated at the bottom (top) of the chart.

lated for each of the intervals and then used to explore the rain type dependent characteristics of the DSDs as a function of rainrate, directly from the experimental integral parameters.

The rainrate dependent variation of the same parameters studied for the rain event in the above example has been analysed in this section, namely, N_0, μ, λ, D_{mean}, σ and N_T. Their variation is displayed in figure 9 and appears to be consistent with the observations of the previous section. For low rain-

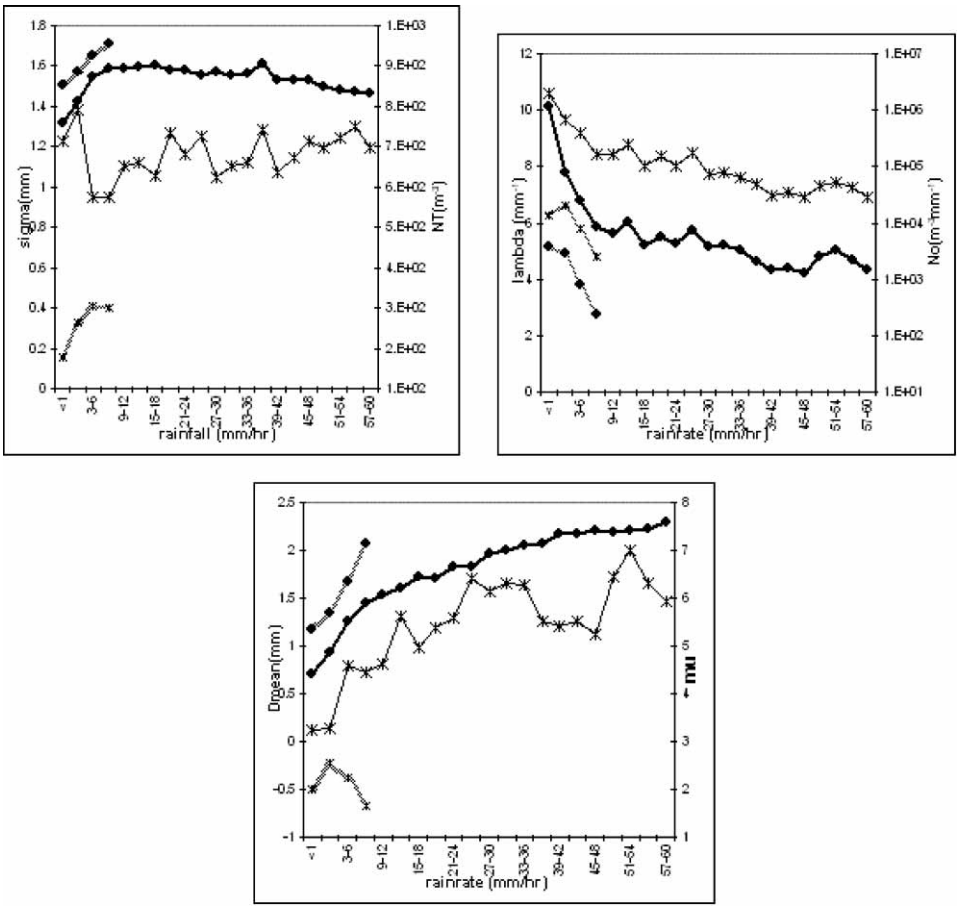

Figure 9. Value of various DSD parameters for all the rain events averaged for every 3 mm/hr as a function of rainrate. (a) D_{mean} (mm) (convective: bold line with full circles, stratiform: grey line with full circles) and μ (convective: line with crosses, stratiform: grey line with crosses) (b) λ (mm^{-1}) (convective: bold line with full circles, stratiform: grey line with full circles) and (m^{-3} mm^{-1}) (convective: line with crosses, stratiform: grey line with crosses) (c) σ (mm) (convective: bold line with full circles, stratiform: grey line with full circles) and N_T (m^{-3}) (convective: line with crosses, stratiform: grey line with crosses)

rates (*i.e.* <10 mm/hr), the average value of λ as well as the parameter μ is smaller for the stratiform rain DSD as compared to convective rainfall. While the above two parameters are not very different for the averaged convective and stratiform rainfall, the mean value of N_0 is very high in the medium convection regime (between 1–9 mm/hr) as compared to stratiform rainfall at similar rainrates. This may be the main reason why; most authors (Waldvogel, 1974; TS, Uijlenhoet, 2003 as well as our results) have observed the N_0 jump in a rainfall event, corresponding to the transition from convective regime to the stratiform regime and vice versa in this range of rainrates, wherein the difference is highest. Many authors have also noted a gradual increase in the value of N_T with rainrate, separately for stratiform and convective rainfall (Atlas et al., 2000) or for all types of rain averaged together (SL). Our study also demonstrates that N_T, as displayed in figure 9, initially decreases and then increases very slowly with rainrate. However, it may be emphasized that this is only the average value. As indicated in the previous section for a particular rain event, the value of N_T may vary considerably independent of the rainrate, both within and between rain events, especially at lower rainrates. So it is difficult to infer any difference between convective and stratiform rainfall from this behaviour of N_T at low rainrates. We also note that the value of D_{mean} as well as σ increases with rainrate for both stratiform and convective rain type, indicating a gradual broadening of the spectrum for both types of precipitation, with larger droplets and broader spectrum predominating in stratiform rain as compared to convective rain DSD. Kollias et al. (1999) have also demonstrated, using a 94-GHz Doppler radar at vertical incidence, similar narrow DSD in convective rain, and a broad spectrum in stratiform rain such as those reported in the present work. This result confirms the fundamentally different form of the DSD spectra for stratiform and convective rainfall.

At still higher rainrates, for convective rainfall, both the slope parameter λ and the intercept parameter N_0, continue to decrease with rainrate, albeit more slowly, especially for rainrates >39 mm/hr. D_{mean} continues to increase with rainrate, although at a slow rate. While the three above parameters tend towards constant value, the value the shape parameter μ continues to rise with the rainrate. As shown in figure 7 as well as figure 9, the variation of N_0 is very similar to that of λ (correlation coefficient 0.94). The high values of N_0 for weak to moderate convective regime and decreasing values for increasing convective activity have previously been observed by several investigators, Waldvogel (1974). The average value of N_T increases very slowly with rainrate while σ starts to decrease with rainrate beyond about 15 mm/hr. When seen in conjunction with the increasing value of D_{mean}, and slow increase in the value of N_T, this indicates increased skewedness of the distribution with increasing rainrate. The slow rate of change of the slope λ of the distribution and the mean mass diameter with rainrate above a threshold rainrate (in this case 39 mm/hr) irrespective of the rain event, is generally in-

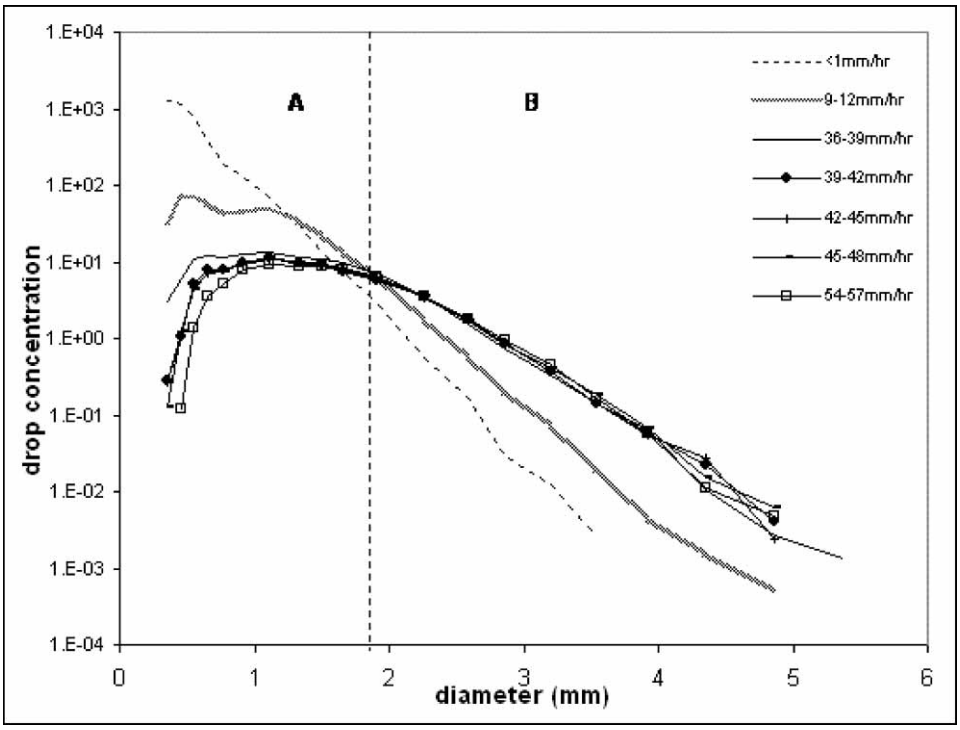

Figure 10. Averaged Drop concentration for various rainrates indicating the gradual tendency towards an equilibrium distribution of convective rainfall. Region A signifies the lower diameter range (<1.91 mm) and region B signifies the higher diameter range (>1.91 mm).

terpreted as attainment of equilibrium form by the convective DSD. Studies in different parts of the world indicate different threshold values for the equilibrium DSD. SL obtained this threshold at about 20 mm/hr, while AU 2000, analysed a particular convective rainfall event and found the equilibrium DSD for values of rainrate as low as 8 mm/hr.

To further analyse the characteristics of the convective DSD, the average DSDs are plotted in figure 10 to indicate the progression of the DSD to an equilibrium shape. For this purpose, each DSD is divided by its rainfall rate, and the »normalized« DSDs so obtained are averaged for each of the rainfall classes. It is observed that the population of droplets decreases in the lower diameter categories while increasing in the higher diameter categories with increase in the rainrate, with the DSD assuming an almost skew symmetric shape. Beyond about 39 mm/hr, the drop population in the higher diameter categories of the DSD attains an almost uniform shape independent of the rainrate, corresponding to the slow rate of change of λ and D_{mean} in figure 9. However, this equilibrium form does not extend to the lower drop diameters within the DSDs. On the basis of the rainrate dependent behaviour of the

DSD, the entire family of DSD has been grouped into two diameter classes. Region A signifies the lower diameter range (<1.91 mm) and region B (>1.91 mm). While the region B attains equilibrium slope above 39 mm/hr as discussed above, the region A does not display any equilibrium shape irrespective of the rainrate.

The sorting of the equilibrium DSDs formed aloft, by the updrafts in the convective clouds has already been discussed in the previous section on the basis of the model proposed by AU 2000 for convective rainfall for the TOGA--COARE experiment. These updrafts modify the DSD formed aloft by the collision-coalescence-breakup-evaporation mechanism of warm clouds and sort the droplets according to size. The larger droplets are less affected by the updraft, which is horizontally convergent, and fall through it so that they reach the surface under the updraft core (Srivastava & Atlas, 1969), while the smaller droplets are pushed upward and outward by the updraft, so that they fall elsewhere. The main effect of the updrafts on large droplets is to increase their residence time in the air, so that the equilibrium distribution for such droplets may be attained at a lesser path length than what was considered necessary by the model of List et al. (1987). This conclusion also fits very well with the observations of SL at other tropical sites, who inferred that; the equilibrium shape for such large droplets (above a threshold defined by them as 1.7 mm, which in our studies is at 1.91 mm) appears to have been reached independent of the drop population in the lower droplet categories.

Our results also display a minimum slope in the DSD at a diameter ~1.0 mm in figure 10. Measurements of vertical velocities at the 3.2 km level by AU 2000 for the TOGA COARE experiment for such convective storms suggested, that the updraft velocities (>4 m/s at 3–5 km) are in the range of the terminal velocities of droplets of this size. This implies that these droplets are held almost in suspension and collision time for such sizes would greatly increase for moderate to strong convective cells. Hence, the distribution observed on the ground as in figure 10, would be most depleted of raindrops in this range of diameters. Our own observation of a plateau region in the DSD in this region validates the above hypothesis. The droplets in the lowest diameter categories, on the other hand, are most sensitive to the balance between the microphysical processes that produce drops and those that delete drops. For example, the concentration of the small drops can be very different in an updraft, where small drops are growing and being replenished by condensation than in a downdraft where they are depleted by evaporation even for the same rainrate (Willis, 1984; Martinez and Gori, 1999). Since the averaged values tend to reflect the variation of the constituent spectra, even at high rainrates, no equilibrium distributions are observed in this range of drop diameters.

The description and inferences of warm convective rain growth, sorting and the effect of updrafts presented above are entirely consistent with observations of warm tropical convective rain in both TOGA-COARE (AU 2000)

and Yuter and Houze (1995) over Florida as well as those of SL for tropical continental rainfall over Africa. In all cases, the 0 °C isotherm was at 4–5 km, as in our observations (4.5 km) (Das, 1988) and there is no reason to believe that the microphysical processes of DSD formation as observed by them are substantially different from our observations.

4. Conclusions

This study presents the results of an analysis of tropical rainfall measured with a JWD over Cuddalore in South India. 4269 samples spread over 16 rain events with varying rainrates have been analysed. The rainrate data corrected for instrumental error, matches very well with a SRRG measured values at 15-minute resolution, placed at the same site. Further results of the observed DSDs are as follows:

1. The gamma fitted DSD were separated into convective and stratiform rainfall categories according to the modified TS algorithm. The value of that separates the DSDs during a rain event into two contiguous groups is much lower than the value obtained by TS for tropical oceanic rainfall. This may have more to do with the method of computation of the integral parameters of the distribution than any real difference in the rainfall producing systems in the two regions. The separation scheme was found to be quite robust, as demonstrated for three different rain events during the season. The temporal continuity as well as correspondence to actual observations of the cloud structure from radar observations is quite good. A 10% change in the value of either the slope or the exponent in the – R relation is observed to cause only about 2–3 % change in the classification scheme.

2. While analysing a particular squall line of 15 September 2002, it is observed that there are distinct differences in DSD between the convective-line and stratiform regions. While the convective region is characterised by sharply skewed DSD spectra centred at higher diameters, stratiform rainfall is of lesser intensity, and the spectra are broader. At the same rainrate, the stratiform spectra have a greater population of large drops (large drop spectra) as compared to convective spectra (small drop spectra). The reflectivity trough region is characterised mostly by small drop spectra.

3. The average DSD for convective rainfall exhibits very high values of N_0 for low and moderate convection (1–9 mm/hr) indicating that the observed » jump« for transition from stratiform to convective rain type will be best observed in this range of rainrates. The value decreases as the rainrate increases, corresponding to the presence of narrow skewed raindrop spectra at higher rainrates for convective rainfall, with larger population of large droplets. In general, for the same rainrate, the average DSD predict broad spectra with significant large drop population for stratiform spectra and narrow small drop spectra for the convective rainfall at similar rainrate. The value of

the shape parameter is very small for stratiform DSD indicating that their shape approaches the two parameter exponential fit.

4. Further analysis of convective spectra at higher rainrates demonstrates a skewed distribution with a tendency towards equilibrium shape beyond 39 mm/hr. The slope of the DSD, the shape parameter, the intercept parameter, as well as the mean mass diameter are observed to become nearly constant while the shape parameter continues to rise with the rainrate. This shape of the distribution at higher rainrates can be explained in terms of the effect of varying vertical velocities on the shape of the equilibrium DSD formed aloft as observed by other investigators in other tropical DSD measurement sites.

Acknowledgements – The authors are grateful to the Director General of Meteorology, India Meteorological Department, for constant encouragement during the course of this study. Thanks are also due to Dr. Donat Hogl of the Distromet Co., Switzerland for promptly providing the original deadtime correction algorithm of Waldvogel (1974) as well as clarifying certain doubts regarding the calibration of the JWD, which created pseudo--peaks in the DSD in early studies. We are grateful to a large number of officers, namely Dr. S. Suresh and Shri S. B. Thampi and Late Shri Rajamani and other staff members working at M. O. Cuddalore and C. W. C. Chennai for providing the JWD and the Doppler weather radar data. The authors thank Dr. Ramesh Kakar, Project Incharge of the Indo--US project and Dr. D. Woolf of NASA,USA. We also thank two anonymous referees for their insightful comments that helped us further improve the paper.

References

Atlas, D. and Chmela, A. C. (1957): Physical synoptic variation of drop-size parameters. Proc. Sixth Weather Radar Conf., Cambridge, MA, Amer. Meteorol. Soc., 21–29.

Atlas, D., Ulbrich, C. W., Marks Jr., F. D., Amitai, E. and Williams, C. R. (1999): Systematic variation of drop size and radar-rainfall relations., *J. Geophys. Res*., **104**, No. D6, 6155–6169.

Atlas, D. and Ulbrich, C. W. (2000): An observationally based conceptual model of warm oceanic convective rain in the tropics. *J. Appl. Meteorol*., **39**, 2165–2181.

Atlas, D., Ulbrich, C. W., Marks Jr., F. D., Black, R. A., Amitai, E., Willis, P. T. and Samsury, C. W. (2000): Partitioning tropical oceanic convective and stratiform rain by draft strength*., J. Geophys. Res.,* **105**, No. D2, 2259–2267.

Biggerstaff, M. I. and Houze Jr., R. A. (1993): Kinematics and microphysics of the transition zone of the 10–11 June 1985 squall-line system. *J. Atmos. Sci.,* **50**, 3091–3110.

Brazier-Smith, P. R., Jennings, S. G. and Lathan, J. (1973): Raindrop interaction and rainfall rates within clouds. Quart. *J. Roy. Meteorol. Soc.*, **99**, 260–272.

Braun, S. A. and Houze Jr., R. A. (1994): The transition zone and secondary maximum of radar reflectivity behind a midlatitude squall line: Results retrieved from Doppler radar data. *J. Atmos. Sci.*, **51**, 2733–2755.

Cataneo, R. and Stout, G. E. (1968): Raindrop-size distributions in humid continental climates and associated rainfall rate-radar reflectivity relationships. *J. Appl. Meteorol.*, **7**, 901–907.

Churchill, D. D. and Houze, R. A. (1984): Development and structure of winter monsoon cloud clusters on 10 December 1978. *J. Atmos. Sci.*, **41**, 933–960.

Das, N. (1988): Mean Monthly Averages (1971–1980) of Radiosonde /Rawin Data for 05:30 hrs IST and 17:30 hrs. IST, India Meteorological Department Publication, DGM, New Delhi, 1988.

Donnadieu, G. (1982): Observation de deux changements des spectres des gouttes de pluie dans une averse de nuages stratiformes. *J. Rech. Atmos.*, **16**, 35–45.

Feingold, G. and Levin, Z. (1986): The lognormal fit to raindrop spectra from frontal convective clouds in Israel. *J. Climate Appl. Meteorol.*, **25**, 1346–1363.

Fujiwara, M. (1965): Raindrop size distributions from individual storms. *J. Atmos. Sci.*, **22**, 585–591.

Heinrich, W., Joss, J. and Waldvogel, A. (1996): Raindrop size distributions and the radar bright band. *J. Appl. Meteorol.*, **35**, 1688–1701.

Heinrich, W., Schmid, W. and Waldvogel, A. (1995): Raindrop size distribution and convection in a midlatitude squall line. Preprints, 27th Int. Conf. on Radar Meteorology, Vail, CO, *Amer. Meteorol. Soc.,* 227–229.

Houghton, H. G. (1968): On precipitation mechanisms and their artificial modification. *J. Appl. Meteorol.*, **7**, 851–859.

Houze, R. A., Jr. (1993): *Cloud Dynamics.*, Academic Press Inc. 573 pp.

Jones, D. M. A. (1992): Raindrop spectra at the ground. *J. Appl. Meteorol.*, **31**, 1219–1225.

Joss, J. and Waldvogel, A. (1967): Ein spektrograph fur Niederschlag tropfen mit automatisher auswertung. *Pure Appl. Geophys.*, **60**, 240–246.

Kollias, P., Lhermitte, R. and Albrecht, B. (1999): Vertical air motion and raindrop size distribution in convective systems using a 94 GHz radar. *Geophys. Res. Lett.*, **26**, 3109–3112.

List, R. and Gillespie, J. R. (1976): Evolution of raindrop spectra with collision induced breakup. *J. Atmos. Sci.*, **33**, 2007–2013.

List, R., Donaldson, N. R. and Stewart, R. E. (1987): Temporal evolution of dropspectra to collisional equilibrium in steady and pulsating rain. *J. Atmos. Sci.*, **44**, 362–372.

Loffler-Mang, M and Joss, J. (2000): An optical disdrometer for measuring size and velocity of hydrometeors. *J. Atmos. Ocean. Tech.*, **17**, 130–139.

Maki, M., Keenan, T. D., Sasaki, Y. and Nakamura, K. (2001): Characteristics of the raindrop size distribution in tropical continental squall lines observed in Darwin, Australia. *J. Appl. Meteorol.*, **40**, 1393–1412.

Martinez, D. and Gori, E. G. (1999): Raindrop size distributions in convective clouds over Cuba. *Atmos. Res.*, **52**, 221–239.

Sauvageot, H. and Lacaux, J. P. (1995): The shape of averaged drop size distributions. *J. Atmos. Sci.*, **52**, 1070–1083.

Sheppard, B. E. (1990): Effect of irregularities in the diameter classification of raindrops by the Joss-Waldvogel disdrometer. *J. Atmos. Ocean. Tech.,* **7**, 180–183.

Smull, B. F. and Houze, R. A. (1987): Dual Doppler analysis of a midlatitude squall line with a trailing region of stratiform rain. *J. Atmos. Sci.*, **44**, 2128–2148.

Srivastava, R. C. and Atlas, D. (1969): Growth, motion and concentration of precipitation particles in convective storms. *J. Atmos. Sci.*, **26**, 535–544.

Srinivasan, V. and Ramamurthy, K. (1973): Post monsoon season over the Indian Peninsula. F.M.U. Rep No. IV–18.4, India Meteorological Department, New Delhi.

Steiner, M., Houze Jr., R. A. and Yuter, S. E. (1995): Climatological characterization of three dimensional storm structure from operational radar and rain gauge data. *J. Appl. Meteorol.*, **34**, 1978–2007.

Stewart, R. E., Marwitz, J. D., Pace, J. C. and Carbone, R. E. (1984): Characteristics through the melting layer of stratiform clouds. *J. Atmos. Sci.*, **41**, 3227–3237.

Tokay, A., Kruger, A., Krajewski, W. F. (2001): Comparison of drop size distribution measurements by impact and optical disdrometers. *J. Appl. Meteorol.*, **40**, 2083–2097.

Tokay, A., Short, D. A., Williams, C. W., Ecklund, W. L. and Gage, K. S. (1999): Tropical Rainfall associated with convective and stratiform clouds: Intercomparison of disdrometer and profiler measurements., *J. Appl. Meteorol.*, **38**, 302–320.

Tokay, A. and Short, D. A. (1996): Evidence from Tropical Raindrop Spectra of the Origin of rain from Stratiform versus Convective clouds. *J. Appl. Meteorol.*, **35**, 355–371.

Ulbrich, C. W. (1983): Natural variations in the analytical form of the raindrop size distribution. *J. Clim. Appl. Meteorol.*, **22**, 1764–1775.

Ulbrich, C. W. and Atlas, D. (1998): Rainfall microphysics and Radar properties: Analysis Methods for drop size spectra. *J. Appl. Meteorol.*, **37**, 912–923.

Uijlenhoet, R., Steiner M. and Smith, J. A. (2003): Variability of Raindrop Size Distributions in a squall line and implications for radar rainfall estimation. *J. Hydrometeorol.*, **4**, 43–61.

Waldvogel, A. (1974): The N_0 jump in raindrop spectra. *J. Atmos. Sci.*, **31**, 1067–1078.

Willis, P. T. (1984): Functional Fits to some observed Drop Size Distributions and Parameterization of Rain. *J. Atmos. Sci.*, **41**, 1648–1661.

Williams, C. R., Ecklund, W. L. and Gage, K. S. (1995): Classification of precipitating clouds in the tropics using 915–MHz wind profilers. *J. Atmos. Ocean. Tech.*, **12**, 996–1012.

Yuter, S. E. and Houze, R. A. (1997): Measurements of raindrop size distributions over the Pacific warm pool and implications for Z–R relations. *J. Appl. Meteorol.*, **36**, 847–867.

Yuter, S. E. and Houze Jr., R. A. (1995): Three dimensional kinematic and microphysical evolution of Florida cumulonimbus. Part III: Vertical mass transport, mass divergence, and synthesis. *Mon. Weather Rev.*, **123**, 1964–1983.

SAŽETAK

Raspodjela kapi tropskih kiša po veličini nad južnom Indijom

Soma Sen Roy, R. K. Datta, R. C. Bhatia i A. K. Sharma

Raspodjela kapi po veličini (RKV) koja je povezana s tropskim kišama u Cuddalore u jugoistočnom dijelu Indije, mjerena je Joss-Waldvogel disdrometrom (model RD-80) od rujna do studenog 2002. Mjerenja kiše su korigirana uvažavajući pogreške instrumenta te se vrlo dobro podudaraju s mjerenjima koja su dobivena automatskom kišomjernom postajom na istoj lokaciji. Radi daljnje analize RKV, količine oborine su podijeljene na konvektivnu i stratiformnu količinu oborine na temelju logaritma koji se zasniva na varijacijama RKV parametara. Jedan slučaj obilne kiše za vrijeme olujne pruge 15. rujna 2002. odabran je za detaljnu analizu radi ispitivanja valjanosti klasifikacijske sheme kao i za proučavanje promjena RKV parametara za vrijeme pomicanja olujne pruge. Pokazalo se da je algoritam robustan i da je imao dobro slaganje s drugim algoritmima za separaciju oborine. Tijekom ispitivanog slučaja, kod malih količina kiše, konvektivnu fazu oborine karakterizira izrazit RKV spektar koji ima veliki broj malih kapljica u odnosu na statiformnu RKV za istu količinu kiše. Za veće količine kiše, konvektivni režim karakterizira uzak spektar velikih kapljica. U području prijelaza između konvektivnog i stratiformnog spektra, uočeno je miješanje velikih i malih kapljica kiše. Slične promjene prisutne su i u spektru srednjih kapljica kiše. Srednji spektar također pokazuje ravnomjernu raspodjelu kapi RKV za veće količine kiše (>39/sat) promjera kapi (>1.91 mm) što odgovara skoro konstantnim vrijednostima nagiba distribucije, presjeka s ordinatnom osi i srednjeg promjera. Vrijednost parametra oblika, koji za male količine kiše varira isto kao i parametar nagiba, počinje

se povećavati s povećanjem količine oborine kao i ostala dva parametra gama razdiobe dosežući konstantnu vrijednost koja odgovara ravnotežnom obliku. Vrijednost presjeka s ordinatnom osi je najviša za male ili umjerene konvektivne količine oborine i smanjuje se s povećanjem količine kiše.

Ključne riječi: Konvektivna kiša, stratiformna kiša, disdrometar, korekcija instrumenta**,** olujna pruga, gama razdioba, sraščivanje kapi, sjedinjavanje kapi, injenje

Corresponding author's address: Soma Sen Roy, India Meteorological Department, Lodi Road, New Delhi – 110003, India, e-mail: somasenroy@yahoo.com